

Non-Equilibrium Superconductivity in Kinetic Inductance Detectors for THz Photon Sensing

D. J. Goldie* and S. Withington*

*Detector and Optical Physics Group

Cavendish Laboratory

University of Cambridge

JJ Thomson Av.

Cambridge

CB3 0HE, UK

Email: d.j.goldie@mrao.cam.ac.uk

Abstract—Low temperature Kinetic Inductance Detectors (KIDs) are attractive candidates for producing quantum-sensitive, arrayable sensors for astrophysical and other precision measurement applications. The readout uses a low frequency probe signal with quanta of energy well-below the threshold for pair-breaking in the superconductor. We have calculated the detailed non-equilibrium quasiparticle and phonon energy spectra generated by the probe signal of the KID when operating well-below its superconducting transition temperature T_c within the framework of the coupled kinetic equations described by Chang and Scalapino.[1] At the lowest bath temperature studied $T_b/T_c = 0.1$ the quasiparticle distributions can be driven far from equilibrium. In addition to the low frequency probe signal we have incorporated a high frequency (~ 1 THz) source signal well-above the pair-breaking threshold of the superconductor. Calculations of source signal detection efficiency are discussed.

I. INTRODUCTION

Kinetic inductance detectors (KIDs) operating at low reduced temperatures $T/T_c \simeq 0.1$, where T is the temperature and T_c is the superconducting transition temperature, are used not only as ultra-sensitive detectors of incident power or individual quanta for applications in sub-millimeter, millimeter, optical, X- and γ -ray astrophysics,[2], [3], [4], [5], [6], [7] but also as elements of Qubits for quantum computing.[8], [9], [10] As a detector the superconductor is formed as a resonator and changes in its complex conductance can be monitored by measuring the complex transmission S_{21} of a probe signal. We recently described a detailed microscopic calculation of the spectrum of the non-equilibrium quasiparticles and phonons in a KID operating at $T/T_c = 0.1$. [11] Prior to that work and despite the technological importance, a detailed microscopic analysis of the effect on the distribution functions of the quasiparticles and phonons at temperatures $T \sim 0.1T_c$ due to the interaction of a *flux* of microwave photons of frequency $\nu_p \ll 2\Delta(T)/h$, where $2\Delta(T)$ is the temperature-dependent superconducting energy gap and h is Planck's constant, seemed to be lacking. By contrast the regime $\nu_p \sim \Delta(T)/h$ with $T \sim T_c$, when gap enhancement effect are predicted and observed, has been extensively studied. The quasiparticles and phonons of a low temperature superconductor form coupled subsystems. Energy relaxation processes of non-equilibrium quasiparticles comprise scattering with absorption or emission of phonons,

and scattering involving Cooper pairs with generation or loss of two quasiparticles and absorption or emission of phonons of energy $\Omega \geq 2\Delta$ respectively. Energy escapes from the superconductor as phonons enter the substrate. The coupled kinetic equations that describe these interacting subsystems were derived by Bardeen, Rickayzen and Tewordt[12] and discussed in detail by Chang and Scalapino.[1], [13] The coupled kinetic equations have been used to investigate the effect of high energy photon interactions ($h\nu_{sig}/\Delta \sim 3 \times 10^7$) at $T/T_c \sim 0.1$. [14], [15]

In Ref. [1] full non-linear solutions were obtained which is the approach we have adopted. Crucially however in that earlier work solutions were obtained close to T_c where microwave drive can lead to gap-enhancement effects. In the present programme our interest lies in the behavior at low effective temperatures, where changes in the quasiparticle density have most effect on the KID. The KID is readout with a microwave probe signal of energy $h\nu_p \ll 2\Delta$ where ν_p is the probe frequency close to the resonant frequency of the KID. Our fundamental observation is that the readout is dissipative, but that there are very few *thermal* quasiparticles present at T_b which can interact with the probe. Our solutions of the coupled kinetic equations showed that the KID can be driven far from equilibrium for typical experimental probe powers.[11] Here we begin to explore the effect of adding a signal power comprising photons of energy $h\nu_{sig} \geq 2\Delta$ so that the signal breaks Cooper pairs in addition to the probe signal for which multiple photon absorption breaks pairs.

An important consideration in the design of a KID for THz photons is the fraction of incident signal power (or indeed energy for single quantum detection) that is coupled to the quasiparticles. The detection geometry we consider would allow the signal to interact directly in the superconductor and so that the signal breaks Cooper pairs. Pair breaking creates excess (primary) quasiparticles, and these quasiparticles scatter to lower energies emitting phonons on a timescale that is on average shorter than the effective population recombination time. These phonons will be lost from the KID if $\Omega < 2\Delta$ but may break additional Cooper pairs if $\Omega \geq 2\Delta$. Pair breaking increases the total number of quasiparticles created by the initial photon interaction and hence the signal that is detected.

Some fraction of the pair-breaking phonons will still be lost from a KID of finite thickness a process which reduces the overall detection efficiency. The probability of pair-breaking is determined by the phonon pair breaking time τ_{pb} and the phonon loss time from the film τ_{loss} . At low temperature and low phonon energies $\tau_{pb} = \tau_0^\phi$ where τ_0^ϕ is the characteristic phonon lifetime.[16]

Kurakado[17] used the equilibrium lifetimes described by Kaplan *et al.*[16] to describe the interaction of a single excess phonon or quasiparticle in a *bulk* superconductor at $T/T_c = 0$ finding that the average energy required to create a quasiparticle was $\epsilon = 1.68\Delta$, or equivalently an efficiency $\eta = 0.59$, where the excess quasiparticles are assumed to have $E = \Delta$. [17] Obviously, because an infinite superconductor is modeled, phonon loss is ignored unless $\Omega < 2\Delta$, and likewise recombination. The effect of a thermal (or even driven) population is likewise ignored since $T/T_c = 0$. Zehnder investigated the interaction of photons of energy ($h\nu_{sig} \sim 3 \times 10^7 \Delta$) in a number of thin film superconductors at $T/T_c = 0.1$ including quasiparticle diffusion and phonon loss although did not extend the modeling to low incident photon energies of interest here.

To our knowledge no solutions of the full coupled equations exist of the efficiency with which monochromatic photons with $h\nu_{sig} \sim 2 - 30\Delta$ create quasiparticles in a thin-film superconductor *including* 2Δ -phonon loss with a probe signal which itself breaks pairs through multiple photon processes.

II. NON-EQUILIBRIUM KIDS

The coupled non-linear equations described by Chang and Scalapino were solved using Newton-Raphson iteration. Details of the scheme, the representation of the quasiparticle and phonon distributions, and the convergence criteria are given in Ref. [11]. In this way non-equilibrium quasiparticle and phonon energy distributions $f(E)$ and $n(\Omega)$ can be calculated. E and Ω are the quasiparticle and phonon energies respectively. An approach to find the drive term of the quasiparticles I_{probe} associated with the probe power was also described, based on the assumption that the absorbed probe power per unit volume P_{probe} can be measured experimentally. Here we adopt a similar approach to calculate the effect of an additional signal power per unit volume P_{sig} .

A. Including a pair-breaking signal

The effect of a signal with photons of energy $E = h\nu_{sig}$ and absorbed power per unit volume P_{sig} can be included in a similar way to the probe signal. The signal contributes an additional drive term to Eq. [2] of Ref. [11] for the quasiparticle distribution function

$$\delta f(E)/\delta t|_{sig} = I_{sig}, \quad (1)$$

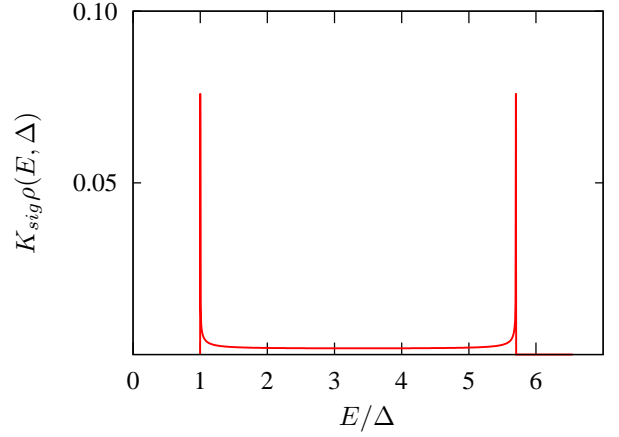


Fig. 1. (Color online) The (number) drive term $K_{sig}\rho(E, \Delta)$ for $h\nu_{sig} = 6.67\Delta$.

where $I_{sig} = B_{sig}K_{sig}$,

$$K_{sig}(E, \nu_{sig}) = 2 \left[\rho(E + h\nu_{sig}, \Delta) \left[1 + \frac{\Delta^2}{E(E + h\nu_{sig})} \right] [f(E + h\nu_{sig}) - f(E)] - \rho(E - h\nu_{sig}, \Delta) \left[1 + \frac{\Delta^2}{E(E - h\nu_{sig})} \right] [f(E) - f(E - h\nu_{sig})] + \rho(h\nu_{sig} - E, \Delta) \left[1 - \frac{\Delta^2}{E(h\nu_{sig} - E)} \right] [1 - f(E) - f(h\nu_{sig} - E)] \right], \quad (2)$$

and the prefactor B_{sig} normalizes the signal power absorption so that

$$B_{sig}(\nu_{sig}) = \frac{P_{sig}}{4N_0 \int_{\Delta}^{\infty} E \rho(E) K_{sig}(E, \nu_{sig}) dE}. \quad (3)$$

In the results discussed later we use as an example a signal with photon energy $h\nu_{sig} = 6.67\Delta$ corresponding to an absorbed frequency $\nu_{sig} = 290$ GHz in Al. Eq. 2 differs from that to describe the probe power in having a third term. This term represents pair-breaking and occurs provided $h\nu_{sig} \geq 2\Delta$. At low temperatures (and low probe powers) this term is the dominant contribution to I_{sig} . Figure 1 shows K_{qp} multiplied by $\rho(E, \Delta)$, thus showing the contribution to the number change, for a pair-breaking signal at low temperatures normalized so that each absorbed photon produces two quasiparticles. The double peak arises because the quasiparticle number generated by pair breaking involves the *product* of final state densities $\rho(E_{sig} - E', \Delta)\rho(E', \Delta)$. The density of states is peaked at $E = \Delta$ and the product is symmetric with respect to the final state energies.

B. KID model parameters

We have used the same parameters to describe the KID given in Ref. [11] which are appropriate for Al. We used

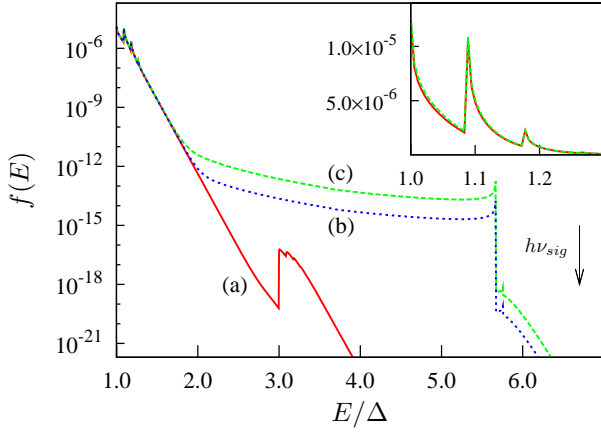


Fig. 2. (Color online) Semi-log plot showing the effect of $P_{probe} = 0.5 \text{ aW}/\mu\text{m}^3$ on the quasiparticle distributions; (a) probe power only (full line red line), (b) $P_{sig}/P_{probe} = 0.01$ (dashed green line) and (c) $P_{sig}/P_{probe} = 0.001$ (dashed blue line) both with the same probe power. The drive photon energy $h\nu_{sig} = 6.67\Delta$ and $\tau_{loss}/\tau_0^\phi = 1$. The inset shows the same $P_{probe} = 0.5 \text{ aW}/\mu\text{m}^3$ and $P_{sig}/P_{probe} = 0.01$ at low energies with a linear ordinate to emphasize the changes.

$\Delta(0) = 180 \text{ } \mu\text{eV}$, $T_c = 1.17 \text{ K}$ and we set $T_b/T_c = 0.1$. The single spin density of states was $N(0) = 1.74 \times 10^4 \text{ } \mu\text{eV}^{-1}\mu\text{m}^{-3}$, characteristic quasiparticle time $\tau_0 = 438 \text{ ns}$ and the characteristic phonon (Debye model) lifetime $\tau_0^\phi = 0.26 \text{ ns}$. [11], [16] In all calculations we assume that the phonon loss can be characterized by a single energy independent time and we assume $\tau_{loss}/\tau_0^\phi = 1$ which we estimate would be appropriate for a 70 nm Al film on Si. [18] We assume a probe photon energy $h\nu_{probe} = 16 \text{ } \mu\text{eV}$, ($\nu_{probe} = 3.88 \text{ GHz}$).

III. RESULTS

Here we show results of the numerical modeling. Fig. 2 shows the calculated non-equilibrium quasiparticle distributions for a probe power of $P_{probe} = 0.5 \text{ aW}/\mu\text{m}^3$ having a probe photon energy $h\nu_p = 16 \text{ } \mu\text{eV}$, as the solid curve and also the additional effect of a pair-breaking signal of power $P_{sig}/P_{probe} = 0.01$ (dashed green curve) and $P_{sig}/P_{probe} = 0.001$ (dashed blue curve). The inset shows a low energy detail of the distributions created by the probe itself and the signal of $P_{sig}/P_{probe} = 0.01$. The main figure shows a number of effects. For the probe signal alone at low energies $E/\Delta \sim 1$ we see the multiple peaked structure corresponding to absorption of the probe signal by the large density of quasiparticles near the gap. At energies $E/\Delta \sim 3$ we see a step in the distribution corresponding to reabsorption of non-equilibrium pair-breaking phonons by the quasiparticles. This structure also exhibits peaks associated with multiple photon absorption from the probe. The distribution functions calculated with an additional pair-breaking signal have similar structure at low energies but show a step in the distribution at $E = h\nu_{sig} - \Delta$. This peak is expected due to the high density of available states at $E = \Delta$, and the curvature of the distribution below this peak arises from the energy dependence of the quasiparticle scattering and recombination

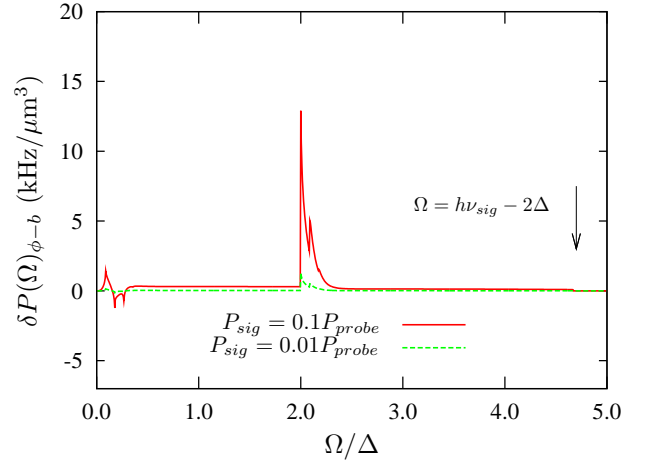


Fig. 3. (Color online) The change in the phonon power flow to the bath $\delta P(\Omega)_{\phi-b}$ for $P_{sig} = 0.1 P_{probe}$ and $P_{sig} = 0.01 P_{probe}$ for $P_{probe} = 0.5 \text{ aW}/\mu\text{m}^3$. The drive photon energy $h\nu_{sig} = 6.67\Delta$ and $\tau_{loss}/\tau_0^\phi = 1$.

rates. The photon peak itself also has a smaller “satellite” peak at $E = h\nu_{sig} - \Delta + h\nu_p$. This arises from absorption of the probe by the quasiparticles created by the signal photons. The inset shows the detail at low energies. It is (just) possible to observe that the distribution with signal is enhanced over that of the probe alone.

Fig. 3 shows the *change* in the phonon power flow to the heat bath after subtraction of that without the signal for two signal powers. We have plotted $\delta P(\Omega)_{\phi-b} = P(\Omega)_{\phi-b}^{sig} - P(\Omega)_{\phi-b}^{probe}$, where $P(\Omega)_{\phi-b}^{sig}$ is the contribution to the phonon-bath power flow with signal and probe, and $P(\Omega)_{\phi-b}^{probe}$ that for the probe alone. The power flow contributions are most easily seen in the plot corresponding to the higher signal power. At low phonon energies $\Omega/\Delta < 0.15$ corresponding to the first probe photon peak there is an increase in the power flow to the bath. At energies $0.15 < \Omega/\Delta < 0.29$ the power is reduced. The first effect is expected as the signal itself has a sharply peaked structure near the gap. The reduction at slightly higher energies is at first sight more surprising but arises from the blocking of final states for the scattering of the higher energy probe-generated quasiparticle peaks towards the gap.

At higher phonon energies there is a significant change in the contribution to the power flow from recombination phonons $\Omega/\Delta \geq 2$ as would be expected for a pair-breaking detection. The energy spectrum also shows a broad low background contribution at all phonon energies $\Omega/\Delta \leq (h\nu_{sig} - 2\Delta)/\Delta$ corresponding to phonons generated by quasiparticle scattering to final state energies $E \sim \Delta$.

IV. PHOTON DETECTION EFFICIENCY

Here we quantify the overall quasiparticle creation efficiency using a simple rate equation approach. We have assumed that an incident monochromatic signal of power per unit volume P_{sig} is absorbed by the quasiparticles. Only a fraction η_{sig} of the absorbed signal supports the excess quasiparticle density N_{ex} because some fraction of the phonons generated in the down-conversion are lost into the substrate.

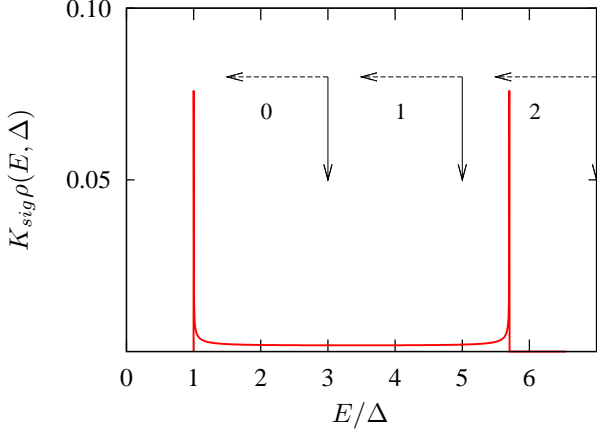


Fig. 4. (Color online) The (number) drive term $K_{sig}\rho(E, \Delta)$ for $h\nu_{sig} = 6.67\Delta$.

During the down-conversion the total number of quasiparticles can however be increased by reabsorption of those phonons which break pairs. If on average each absorbed signal photon generates m_{sig} additional quasiparticles then the sum of the rates of generation by photons and loss by phonon processes is given by

$$\frac{\delta N_{qp}^{ex}}{\delta t} = m_{sig} \frac{\delta N_{sig}}{\delta t} + \left. \frac{\delta N_{qp}^{ex}}{\delta t} \right|_{\phi}. \quad (4)$$

In steady state $\delta N_{qp}^{ex}/\delta t = 0$ and we use $N_{qp}^{ex} = 4N_0 \int_{\Delta}^{\infty} \rho(E)(f_{sig} - f_p)dE$. The rate of photon absorption from the signal is $\delta N_{sig}/\delta t = P_{sig}/h\nu_{sig}$. The loss rate due to phonons is $\delta N_{qp}^{ex}/\delta t|_{\phi} = -N_{qp}^{ex}/\tau_r^{eff}$ so we have

$$m_{sig} = \frac{h\nu_{sig} 4N_0 \int_{\Delta}^{\infty} \rho(E)(f_{sig} - f_p)dE}{P_{sig} \tau_r^{eff}}, \quad (5)$$

where $\tau_r^{eff} = \tau_r^{sig}/2(1 + \tau_l/\tau_{pb})$ is the effective recombination time for the driven population with the signal. We find that $m_{sig} = 3.29$ for $h\nu_{sig} = 6.67\Delta$ giving a number detection efficiency $\eta_n = 3.29\Delta/6.67\Delta = 0.49$ if we assume that all of the signal-generated excess quasiparticles in static non-equilibrium have $E = \Delta$. In a similar way we can calculate the power detection efficiency

$$\eta_{sig} = \frac{4N_0 \int_{\Delta}^{\infty} E\rho(E)(f_{sig} - f_p)dE}{P_{sig} \tau_r^{eff}} \quad (6)$$

giving $\eta_{sig} = 0.51$ and here we have taken account of the energy distribution of the excess quasiparticles.

V. DISCUSSION AND CONCLUSIONS

We have presented preliminary calculations of the detailed energy spectra of the non-equilibrium quasiparticles and phonons of a representative and technologically interesting low temperature superconductor (here Al) generated by a low power pair-breaking signal of frequency $\nu_{sig} = 290$ GHz. Considering the energy relaxation processes within the superconductor the calculation is fully representative of photon absorption up to $h\nu_{sig} = \Omega_D$ where Ω_D is the Debye energy,

and for reference $\Omega_D \sim 8$ THz. The model includes a higher power probe of frequency $\nu_{probe} \sim 4$ GHz chosen to be typical of the powers and frequencies used in KID readout. The detailed spectra show the effects of interaction between the probe and the signal showing structure for example at $E = h(\nu_{sig} + \nu_{probe})$. In future work we will extend the model to investigate the detection linearity of a resonator with the driven distributions. It will also be possible for example to calculate the behaviour of the resonator used as a mixer.

We calculated the effective population quasiparticle lifetime for the driven distribution and used a simple rate equation approach to find the static driven number of quasiparticles generated by the high frequency signal. In this way a number detection efficiency $\eta_{sig} \sim 0.5$ was found for a signal of frequency $\nu_{sig} = 290$ GHz assuming a phonon loss time $\tau_{loss}/\tau_0^{\phi} = 1$. This efficiency may seem at first sight low. Figure 4 presents a naive model to understand the energy down-conversion and appreciate the calculated detection efficiency. The curve reproduces the quasiparticle number spectrum generated by a single interacting signal photon shown in Fig. 1. The vertical arrows at 3, 5 and 7 Δ are intended to break the number spectrum into regions labeled 0, 1 and 2 respectively. In the simplest approximation we would assume that quasiparticles relax by scattering i.e. ignoring recombination. The group of quasiparticles in region 0 have energies below 3 Δ . On scattering to lower energies, predominantly $E = \Delta$, they emit phonons of energy $\Omega < 2\Delta$ which are lost from the film. Scattering of this group does not change the static number density merely the spectrum. Quasiparticles in region 1 have energies $3\Delta < E < 5\Delta$. On scattering to lower energies, these emit secondary phonons of energy $2\Delta < \Omega < 4\Delta$. These may break pairs and the probability of pair breaking over all possible phonon processes is $p = \tau_{loss}/(\tau_{loss} + \tau_{pb})$. Ignoring the energy dependence of τ_{pb} then $p = 0.5$, (in this approximation $\tau_{pb} = \tau_0^{\phi}$ [16]), so that a fraction of the power generating these quasiparticles would be lost from the film during the down-conversion. A similar discussion would apply to region 3 but now the secondary phonons with $4\Delta < \Omega < 6\Delta$ create secondary quasiparticles with energies $3\Delta < E < 5\Delta$ and probability p . These in turn scatter and create tertiary pair-breaking phonons of which a fraction p create additional pairs. The overall probability of this process is reduced ($p' = p^2$). We have not as yet set up a detailed model of this process within this framework. This would need to include not only the energy dependence of $\tau_{pb}(\Omega)$ but also the spectrum of phonons generated as the primary quasiparticle spectrum relaxes and the resultant spectrum of the secondary quasiparticles. To an extent this extended (naive) calculation should begin to approximate the detail contained in the full non-equilibrium solutions already described. Even so, using even the very simplest approach, approximating the spectrum of Fig. 4 by δ -functions at $E = \Delta$ and $E = h\nu_{sig} - \Delta$, we estimate $\eta \sim 0.52$ in excellent agreement with the full non-equilibrium calculation and we would expect recombination to reduce this estimate. For higher incident photon energies we would expect this efficiency to be further reduced.

We believe that the model we have described and in particular the detection efficiency of thin-film superconductors in the THz regime has important consequences. If the quasiparticle creation efficiency is as we have described, the achievable sensitivity, or equivalently noise equivalent power of KIDs used for this application in the geometry considered may be compromised, certainly if earlier published estimates are used which ignore phonon loss from thin films.

REFERENCES

- [1] J. J. Chang and D. J. Scalapino, "Nonequilibrium superconductivity," *J. Low Temp. Phys.*, vol. 31, pp. 1–32, 1978.
- [2] P. K. Day, H. G. LeDuc, B. A. Mazin, A. Vayonakis, and J. Zmuidzinas, "A broadband superconducting detector suitable for use in large arrays," *Nature*, vol. 425, pp. 817–821, 2003.
- [3] J. Zmuidzinas, "Superconducting Microresonators: Physics and Applications," *Ann. Rev. Condens. Matter Phys.*, vol. 3, pp. 169–214, 2012.
- [4] G. Vardoulakis, S. Withington, and D. J. Goldie, "Superconducting kinetic inductance detectors for astrophysics," *Meas. Sci. Technol.*, vol. 19, p. 015509, 2008.
- [5] A. Monfardini, L. J. Swenson, A. Bideaud, F. X. Desert, S. Doyle, B. Klein, M. Roesch, C. Tucker, P. Ade, M. Calvo, P. Camus, C. Gior-dano, R. Guesten, C. Hoffmann, S. Leclercq, P. Mauskopf, and K. F. Schuster, "NIKA: A millimeter-wave kinetic inductance camera," *Astron. Astrophys.*, vol. 521, p. A29, 2010.
- [6] J. J. A. Baselmans, "Kinetic Inductance Detectors," *J. Low Temp. Phys.*, vol. 167, pp. 292–304, 2011.
- [7] P. J. de Visser, J. J. A. Baselmans, S. J. C. Yates, P. Diener, A. Endo, and T. M. Klapwijk, "Microwave-induced excess quasiparticles in superconducting resonators measured through correlated conductivity fluctuations," *Appl. Phys. Lett.*, vol. 100, p. 162601, 2012.
- [8] L. DiCarlo, M. D. Reed, L. Sun, B. R. Johnson, J. M. Chow, J. M. Gambetta, L. Frunzio, S. M. Girvin, M. H. Devoret, and R. J. Schoelkopf, "Preparation and measurement of three-qubit entanglement in a superconducting circuit," *Nature*, vol. 467, pp. 575–578, 2010.
- [9] M. Hofheinz, E. M. Weig, M. Ansmann, R. C. Bialczak, E. Lucero, M. Neeley, A. D. O'Connell, H. Wang, J. M. Martinis, and A. N. Cleland, "Generation of Fock states in a superconducting quantum circuit," *Nature*, vol. 454, pp. 310–314, 2008.
- [10] R. V. Schoelkopf and S. M. Girvin, "Wiring up quantum systems," *Nature*, vol. 451, pp. 664–669, 2008.
- [11] D. J. Goldie and S. Withington, "Non-equilibrium superconductivity in quantum-sensing superconducting resonators," *Supercond Sci and Tech*, vol. 26, p. 015004, 2013.
- [12] J. Bardeen, G. Rickayzen, and L. Tewordt, "Theory of the thermal conductivity of superconductors," *Phys. Rev.*, vol. 113, pp. 982–994, 1959.
- [13] J. J. Chang and D. J. Scalapino, "Kinetic-equation approach to superconductivity," *Phys. Rev. B*, vol. 15, pp. 2651–2670, 1977.
- [14] A. Zehnder, "Response of superconducting films to localized energy deposition," *Phys. Rev. B*, vol. 52, pp. 12 858–12 866, 1995.
- [15] K. Ishibashi, K. Takeno, T. Nagae, and Y. Matsumoto, "Output signal from Nb-based tunnel junctions by irradiation of 6 keV X-rays," *IEEE Trans. Magnetics*, vol. 27, pp. 2661–2664, 1991.
- [16] S. B. Kaplan, C. C. Chi, D. N. Langenberg, J. J. Chang, S. Jafarey, and D. J. Scalapino, "Quasiparticle and phonon lifetimes in superconductors," *Phys. Rev. B*, vol. 14, pp. 4854–4873, 1976.
- [17] M. Kurakado, "Possibility of high resolution detectors using superconducting tunnel junctions," *Nucl. Instrumen. Methods*, vol. 196, pp. 275–277, 1982.
- [18] S. B. Kaplan, "Acoustic matching of superconducting films to substrates," *J. Low Temp. Phys.*, vol. 37, pp. 343–365, 1979.